The influence of helium on deuterium retention in beryllium co-deposits

Anže Založnik[a], Matthew J. Baldwin[b], Russell P. Doerner[b], Thomas Schwarz-Selinger[c], Sebastijan Brezinsek[d]

[a] *Jozef Stefan Institute, Jamova cesta 39, 1000 Ljubljana, Slovenia*
[b] *Center for Energy Research, University of California at San Diego, 9500 Gilman Dr, La Jolla, CA 92093, USA*
[c] *Max-Planck-Institut für Plasmaphysik, Boltzmannstrasse 2, D-85748 Garching, Germany*
[d] *Forschungszentrum Jülich GmbH, Institut für Energie und Klimaforschung - Plasmaphysik, 52425 Jülich, Germany*

Abstract

Tritium co-deposition with materials from the plasma-facing components is expected to be the main contributor to tritium retention in ITER. Since He will also be present in the plasma as fusion ash during the DT campaign, this study focuses on the effect of He on D retention in Be co-deposits. The PISCES-B linear plasma device was used to create co-deposited Be-D-He layers for various deposition temperatures (295 K - 475 K) and He concentrations in $D - \alpha He$ plasma mixtures ($0 \leq \alpha \leq 0.1$). Thermal desorption spectroscopy and nuclear reaction analysis were used to determine the D concentration in co-deposits. For the lowest He concentration (1%) an increase of D retention was observed for the deposition at room temperature, whereas for higher He concentrations a declining trend of D retention was found. Including 10% of He in the plasma is found to reduce D retention at deposition temperatures below 425 K and have a negligible effect at higher deposition temperatures.

Keywords:
D retention, Be co-deposits, helium

Email address: anze.zaloznik@ijs.si (Anže Založnik)

1. Introduction

Tungsten (W) and beryllium (Be) are the materials of choice for the ITER divertor and first wall, respectively. Due to the plasma-wall interaction the material will be eroded and re-deposited together with other species present in the vessel, such as deuterium (D), tritium (T) and helium (He). Experiments from the JET-ILW show that Be rich co-deposits formed mostly on the cold surfaces of the inner divertor, where the surface temperature reaches around 373 K [1]. Moreover, the WallDYN [2] code for impurity migration and wall composition dynamics was used to predict Be deposition patterns and the resulting co-deposition for ITER [3]. The calculation predicts significant Be deposition on inner and outer divertor baffles, where the predicted surface temperature is around 388 K [4], according to calculations performed with SOLPS 4.3 code package [5]. However, extrapolation from JET-ILW to ITER is not straigthforward and simulation results depend strongly on the assumptions of ITER design and operation conditions.

Co-deposition is expected to be the main mechanism contributing to the long-term retention of the fusion fuel [6]. Since fuel retention presents a safety issue due to the radioactive nature of T, a safety limit of in-vessel T has been set to 1 kg [7] and a number of T removal techniques has been proposed in the case of ITER. To address T retention and removal issues, many studies on D retention and/or release behavior from Be-D co-deposits [8, 9, 10, 11, 12] have been performed. However, there is a limited number of studies on the effect of He co-deposition on hydrogen isotope retention. A low concentration of He (up to 6% of He in ITER [13]) will be present in the vessel as an ash from the D-T fusion reaction and moreover, ITER will operate with He/H plasma mixture during the Pre-Fusion Power Operation (PFPO) phase [14]. It has been shown that inclusion of He in D plasma reduces D retention in bulk Be exposed to $D-He$ plasma mixture [15, 16]. The aim of the current study is to investigate the influence of He on D retention in Be-D-He co-deposits.

2. Experiment

The PISCES-B linear plasma device [17] was used to produce ten co-deposited Be-D-He layers. Each layer was produced under different deposition conditions varying the substrate temperature between 300-475 K and He concentration in the $D-\alpha He$ plasma ($0 \leq \alpha \leq 0.1$). Helium concentration was not monitored by optical spectroscopy during the experiment, however

it was controlled by setting the pressure of He gas according to [18], where He concentration in $D - \alpha He$ plasma mixture was calibrated by He I (447.1 nm) optical emission spectroscopy for different He gas pressures. Deuterium partial pressure was kept constant for all plasma mixtures.

A S-65 Be target (made by The Peregrine Falcon Corporation) with a diameter of 25 mm and a thickness of 1.5 mm was exposed to pure D or a mixture of D and He plasma. The plasma parameters were similar for all exposures and were measured by a Langmuir probe close to the target. The electron density and temperature were $(2-3) \times 10^{18}$ m^{-3} and $(4-5)$ eV, respectively. The ion flux was $(1.5-2.5) \times 10^{22}$ m^{-2}s^{-1} and the floating and the plasma potential were around -30 V and -20 V, respectively. The Be target was biased to -120 V to keep the energy of the impacting ions at $\approx$ 100 eV. The target temperature was measured at the rear by a thermocouple and varied between 300 K and 800 K. Since Be erosion yield is constant in this temperature range [19], the formation of co-deposits is not influence by this variation of the temperature.

Co-deposits were collected on circular polished W substrates with a diameter of 20 mm and a thickness of 1 mm, cut in two identical halves. The average Be deposition rate was 0.07×10^{15} Be/cm^{2}s, resulting in the average layer thickness of 15 nm, which was calculated assuming the atom density of bulk Be. The substrates had a direct line of sight towards the Be target and were shielded from the direct interaction with the plasma. They were kept at a constant temperature during the deposition. The deposition probe, holding the substrates, is fully retractable into a vacuum interlock chamber [20]. This allowed substrates to be inserted into position for deposition only after stationary plasma conditions were achieved. The main contributions to co-deposited layers are believed to be D and He reflection from the target and sputter erosion of the Be target [9]. A scheme of experimental setup is shown in Fig. 1.

Every deposition procedure resulted in identical co-deposits on two halves of the W substrate. One was used for thermodesorption spectroscopy (TDS) and another for nuclear reaction analysis (NRA). The TDS analysis was performed in a quartz tube attached to a stainless steel vacuum chamber with a background pressure in a range of 10^{-7} mbar [11]. Each sample was linearly heated by an infrared heat source up to 1273 K at a rate of 18 K/min. Partial pressures of desorbing species were recorded by two residual gas analyzers (RGA). The first is a wide range RGA used to follow species of a mass up to 46 m/q. The second is a high resolution 0-6 m/q RGA

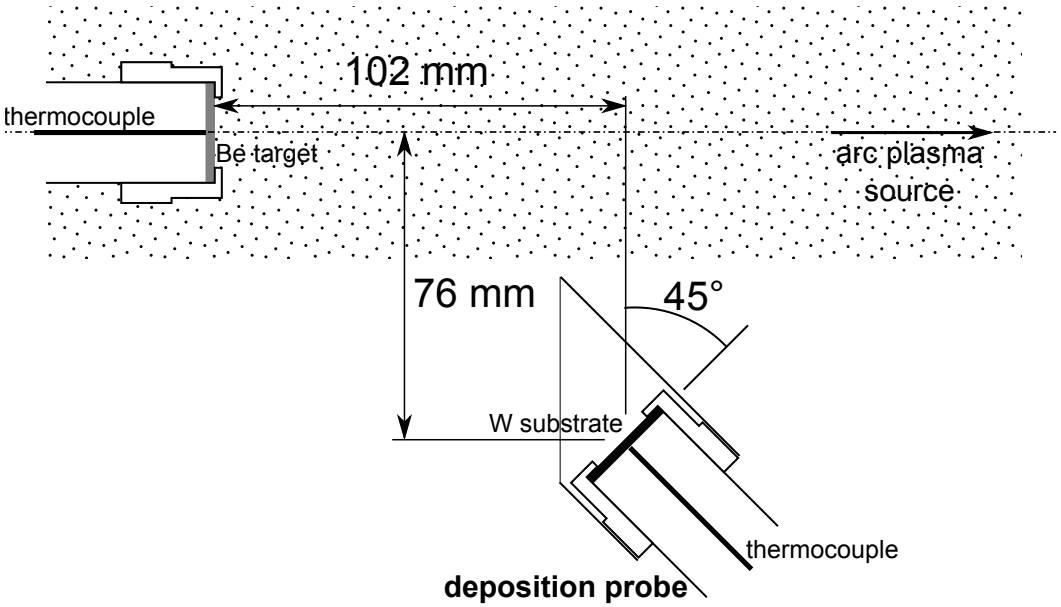

Figure 1: A scheme of experimental setup.

capable of distinguishing between He and D_2. It was used to follow the partial pressures of H_2, HD, He and D_2. Both RGAs were calibrated with D_2 and He leak standards, enabling the conversion of the RGA signal to atomic desorption flux. The sensitivity for D_2 and HD was assumed to be the same.

The total D and Be amounts were determined by NRA technique utilizing $D(^3He, p)^4He$ and $^9Be(^3He, p)^{11}B$ nuclear reactions. A ^3He probing ion beam with the energy of 2.0 MeV and 0.8 MeV was used and the number of reaction protons with respect to their energy was measured. The measured proton yields were converted in areal densities by comparing the signals with those derived from calibration samples. For D a 274 nm thick, plasma-deposited amorphous, deuterated carbon thin film on silicon was used and for Be a 680 nm thick, magnetron sputtered film on silicon was used. After NRA analysis the samples were used for additional TDS analysis, since the effect of NRA

on D and He amount in the sample is negligible.

3. Results

Fig. 2 shows D desorption fluxes from Be co-deposits exposed to pure D plasma and a mixture of $D - 10\%He$ plasma for various deposition temperatures measured by high resolution RGA. The desorption spectra were obtained by adding together the mass 4 (D_2) and a half of the mass 3 (HD) spectra and dividing by the area of the co-deposit and areal density of Be atoms established from NRA analysis, enabling us to compare co-deposited layers with small variations of the layer thickness. A sharp desorption peak with a long high temperature tail arises around 500 - 530 K for the samples deposited at room temperature. For higher deposition temperatures the desorption moves to higher temperature. In the case of the highest deposition temperature, 475 K, the sharp peak is absent and only the 'tail' is visible.

Comparison between Figs. 2(a) and 2(b) reveals much lower D desorption in the case of $D - 0.1He$ plasma compared to pure D plasma. In the case of deposition at room temperature the peak height decreased by 57%. For higher deposition temperatures the difference in the peak height is reduced, the peaks decreased by 40% and 34% for 375 K and 425 K, respectively. In the case of 475 K the difference in the peak height is less than 1%.

For the deposition at room temperature the He concentration in $D-\alpha He$ plasma was also varied. Fig. 3 shows D desorption spectra for $\alpha = 0$, 0.01, 0.05 and 0.1. One can see almost the same peak height for the lowest three He concentrations and a strong decrease in the case of $\alpha = 0.1$. In addition, the peak shifts for ≈ 30 K to lower desorption temperatures in the case of the highest He concentration. However, one should note that small temperature uncertainties arise from the measurement errors during TDS and during plasma exposure.

In order to determine D/Be ratios the total D amounts were first determined by integrating the TDS spectra over time. In addition, areal densities of both, D and Be atoms were measured by NRA technique. The D/Be ratios are shown in Fig. 4 where two sets of data are presented, one showing the average D concentrations determined by TDS and the other showing D concentrations measured by NRA. All D amounts were divided by the Be areal density, determined by NRA. Both techniques are in good agreement with the average difference between TDS and NRA data of approximately 6%.

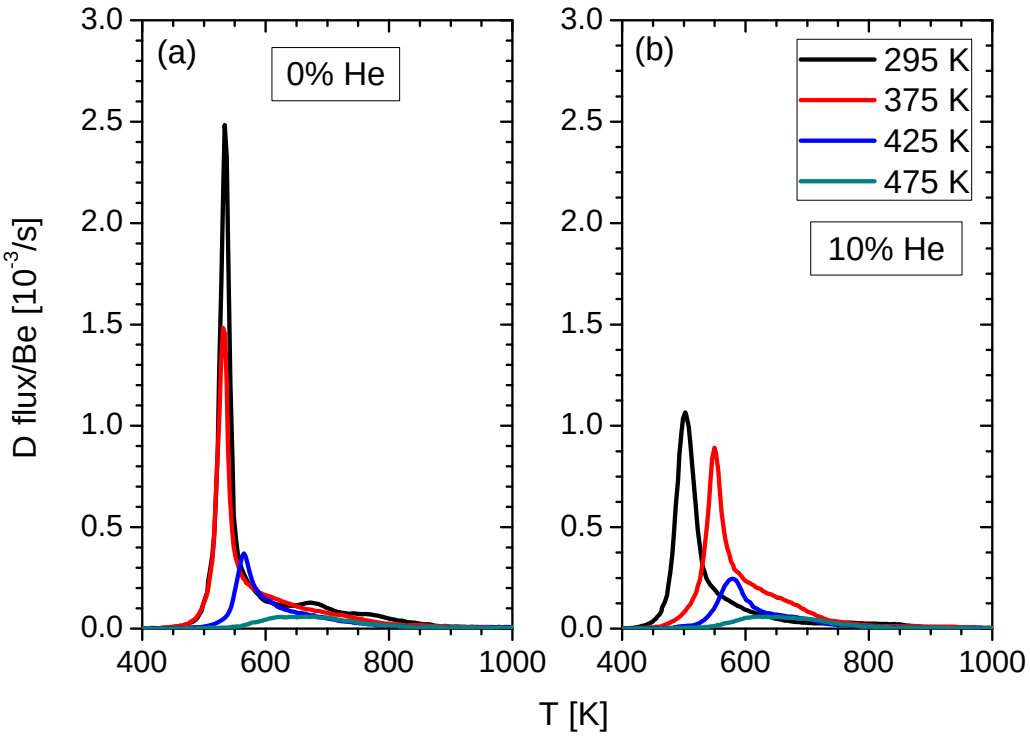

Figure 2: Scaled deuterium desorption spectra of Be-D-He co-deposits for different deposition temperatures and (a) pure D and (b) $D - 0.1He$ plasma.

The D/Be uncertainties are determined as the root sum square of the calibration bottle uncertainty and standard deviation of the background noise in the case of TDS data and as the standard deviation of the counting statistics in the case of NRA data.

The inclusion of 10% He in D plasma reduces D retention by 21% and 36% in the case of deposition at 295 K and 375 K, respectively. For higher deposition temperatures 10% of He does not noticeably affect D retention. The effect of lower He concentrations was measured only for the deposition at room temperature. An initial 17% increase of D retention was measured for the inclusion of 1% He in the plasma mixture, whereas for higher He concentrations D retention is reduced. The retention in the case of 5% He plasma is still 9% higher compared to the pure D plasma, however the uncertainties

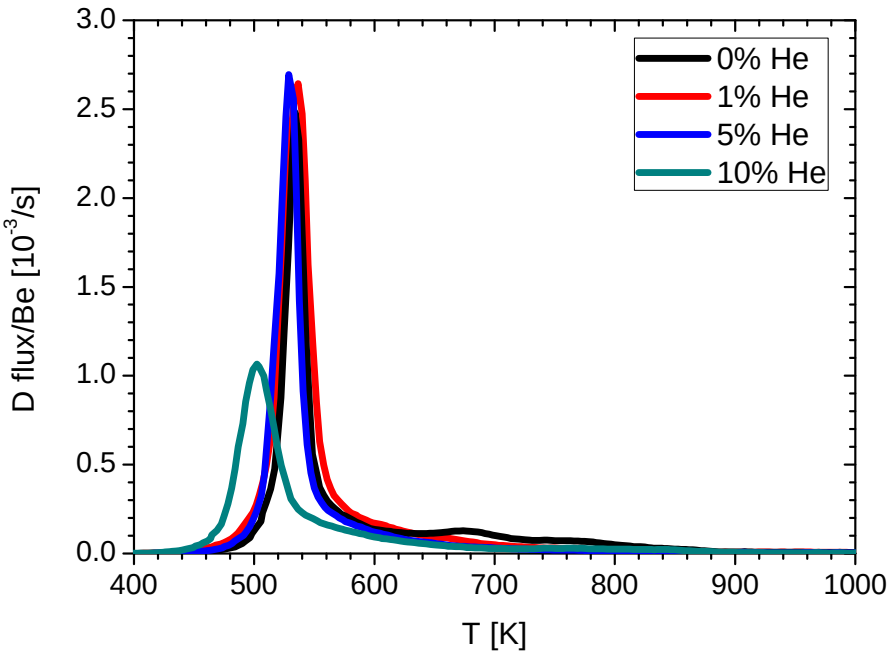

Figure 3: Scaled deuterium desorption spectra of Be-D-He co-deposits for different He concentrations in $D - \alpha He$ plasma and deposition at room temperature.

of these two data points largely overlap.

The high resolution RGA enabled us to distinguish between D_2 and He peaks in the mass spectra. However, the He peak resides on the long tail of a usually stronger D_2 peak in the RGA spectra. Therefore, a time evolution of a measured He signal is a superposition of a real He signal and a background with a shape of D signal. For the background subtraction we scaled the previously determined D signal to the measured He signal and subtracted the resulting scaled D signal. After the subtraction we are left with the real He signal without the D_2 induced background.

Fig. 5 shows He desorption spectra after the background subtraction. No desorption was observed in the case of pure D plasma, as well as in the case of $D-0.1He$ plasma for the deposition at room temperature. For $D-0.1He$ plasma and higher deposition temperatures, 375 K and 425 K, two sharp

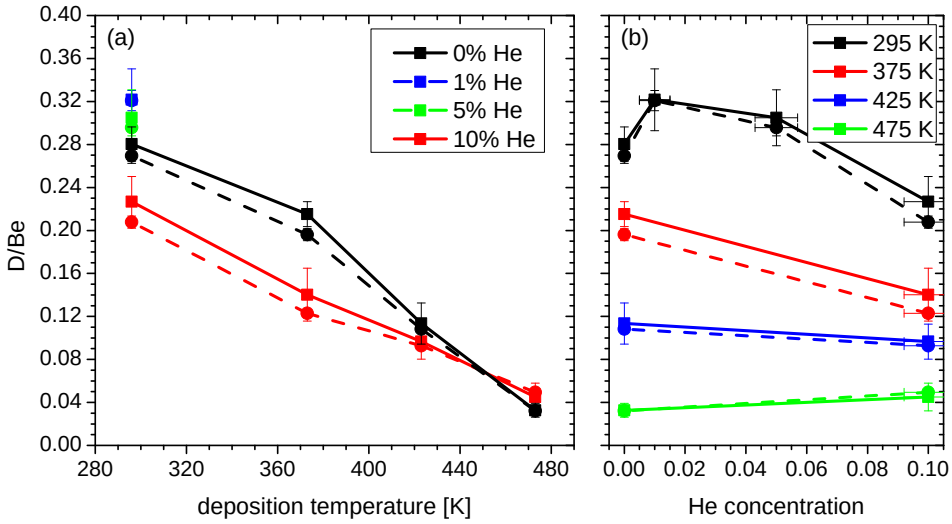

Figure 4: D/Be as a function of (a) deposition temperature for different $D-\alpha He$ plasmas and as a function of (b) He concentration in the plasma for different deposition temperatures. Squares with solid lines represent TDS data and circles with dashed lines represent NRA data. The He concentration uncertainties are estimated from the uncertainties of the data presented in [18].

He desorption peaks were observed. The first peak position is the same for both deposition temperatures being 500 K, whereas the second peak shifts from 920 K for lower to 940 K for higher deposition temperature. Moreover, the height of the first peak decreases, whereas the second peak is strongly enhanced for higher deposition temperature. In addition, weak He desorption can be seen around 750 K. In the case of deposition at 475 K both peaks are strongly reduced compared to deposition at 375 K and 425 K, however the desorption at 750 K is enhanced and a new peak is formed.

Integrating the He desorption spectra and dividing by Be areal density, determined by NRA, gives us the average He atomic fraction in the layers shown in Fig. 6. A very small or zero amount of He was found for deposition at room temperature regardless of He concentration in $D-\alpha He$ plasma. As expected, He concentration in the co-deposited layers is zero within the uncertainties in the case of pure D plasma. The non-zero values are measured only due to the overlap of He and D_2 signals. In the case of $D-0.1He$ plasma

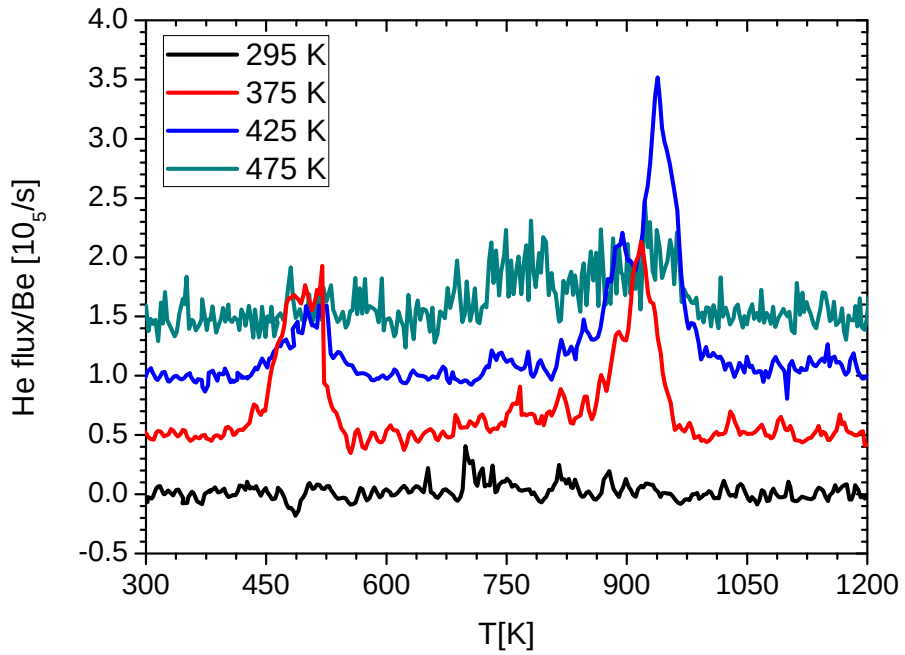

Figure 5: Scaled helium desorption spectra of Be-D-He co-deposits for $D - 0.1He$ plasma and different deposition temperatures. Spectra are successively offset by 5×10^{-6} s^{-1}.

the He content in the layers strongly increases with deposition temperature up to 425 K. For deposition at 475 K He concentration is again reduced, being similar to the concentration measured for deposition at 375 K.

4. Discussion

De Temmerman et al. [9] reported on deuterium retention in co-deposited beryllium layers and derived an empirical scaling law that allows to calculate the D/Be ratio from the deposition temperature, growth rate and particle energy. A comparison of the predicted D concentration with our results obtained using pure D plasma yields an overestimation by the scaling law by a factor of 2-7. The reason for this disagreement is not completely clear since the same setup and similar conditions were used in both cases. The only noticeable difference is in the neutral pressure and ion flux to the Be

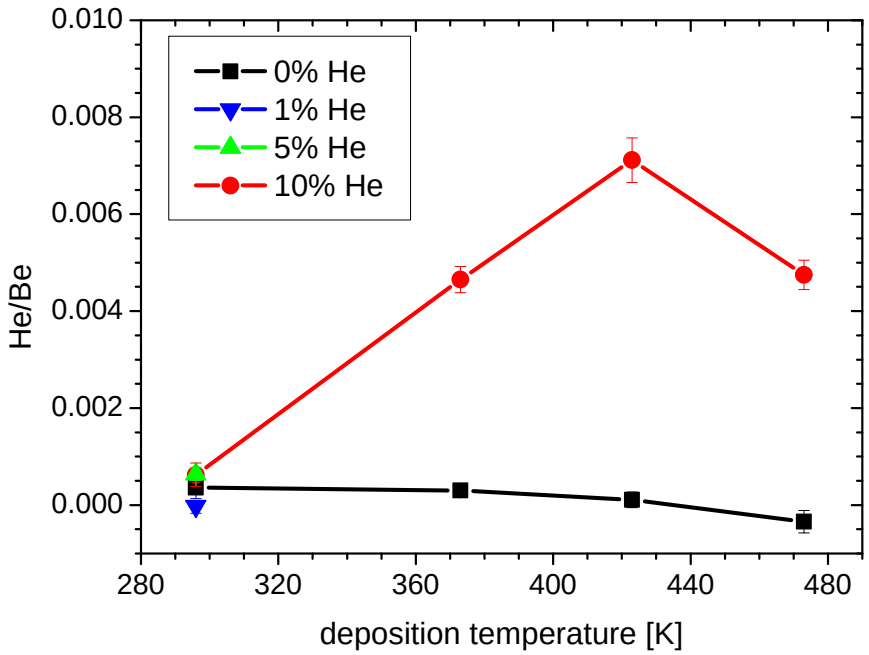

Figure 6: He/Be dependence on deposition temperature for different $D - \alpha He$ plasmas. The error bars represent the root sum square of the calibration bottle uncertainty and standard deviation of the background noise in the TDS signal.

target, both being lower in our case. The De Temmerman scaling considers the beryllium deposition rate, the average energy of the backscattered D particles and the deposition temperature to predict D retention in a Be-D layer, therefore the difference in the ion flux should be indirectly accounted for by the deposition rate. Moreover, as shown in [21] the scaling successfully predicts D retention for various neutral pressures. However, as shown in Fig. 7, we found a much better agreement with the revised scaling law, presented in [10]. In this scaling the Be deposition rate is replaced by the ratio of D and Be fluxes to the substrate plate. For the derivation of the scaling both fluxes are estimated using the data from [22]. In our case we used the same procedure to estimate the D flux, whereas the experimentally determined deposition rate was used as the Be flux. The average energy of the backscattered D particles was calculated in the same way as in [9, 10],

using the data from [22].

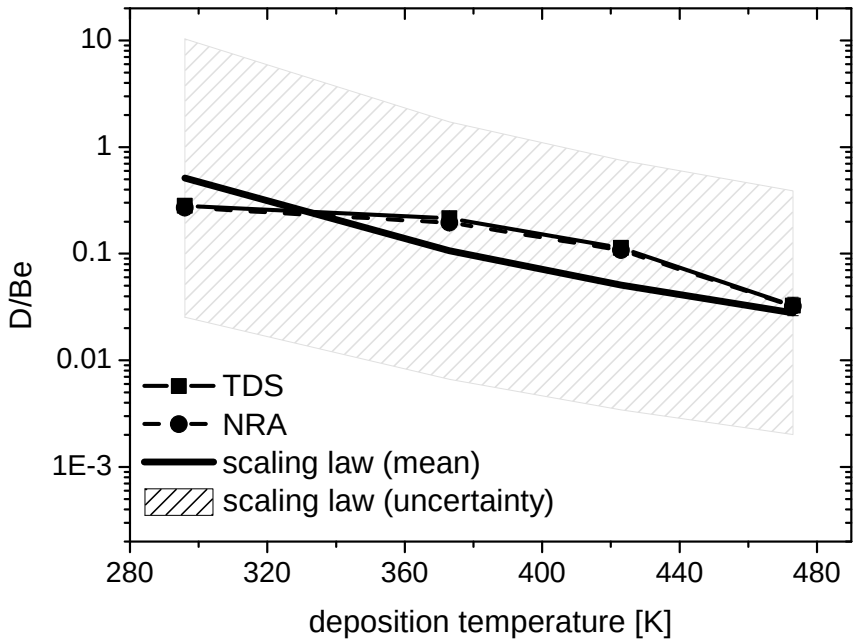

Figure 7: Comparison of D/Be determined by the current experiment with the pure D plasma and the scaling law [10].

The study by Baldwin et al. [15] showed that the admixture of He in D plasma reduces D retention in bulk Be. A threefold reduction of D retention was measured in the case of exposure at 300 K and 10% of He in the plasma. For higher exposure temperatures the difference in D retention between pure D and $D - 0.1He$ plasma diminished and was not apparent above 475 K. Fig. 4 shows similar behavior of D retention in Be co-deposits, however the effect of He admixture to D plasma is smaller compared to data in bulk Be. The reduction of only 1.3 was observed in the case of deposition at room temperature. Similarly to bulk Be the effect of He is reduced at higher deposition temperatures and is not evident above 425 K.

Similarly, in a study by Alegre et al. [16] a 55% reduction of D retention was observed in bulk Be exposed to $D-0.1He$ plasma at 373 K compared to

exposure to pure D plasma. Again, the effect in Be co-deposits is smaller, the reduction of D retention being 36% for the deposition at 375 K. Moreover, in [16] the authors report a negligible effect on D retention when adding 5% of He in the plasma in the case of higher exposure temperatures (473 K to 773 K). In the case of exposure at 373 K a 40% reduction of D retention was observed, however, the data points corresponding to $D - 0.05He$ and pure D plasma are very similar within their uncertainties for all exposure temperatures. With that in mind, this result agrees with our observation where adding 5% of He in the plasma doesn't significantly affect the co-deposited D amount in Be, however, our measurement was only performed at room temperature.

The mechanism by which He influences D retention in co-deposited Be layer is not clear. A post-mortem transmission electron microscope analysis of an inner divertor tile from JET-ILW (where no He was present) shows the presence of bubbles in the Be-rich co-deposited layers [23], however no interconnection between the bubbles has been reported. On the other hand, He ion implantation in bulk Be can lead to a creation of interconnected bubbles and channels, as shown in [24]. Therefore, a possible explanation for the reduced D retention in the presence of higher He concentration could be a He-assisted creation of such interconnected bubbles. Since these structures can easily extend to the surface, they provide an escape path for both, D and He, which can result in lower D retention. At elevated temperatures D ion implantation in bulk Be, similarly as He ion implantation, also results in cavities forming complicated labyrinth systems which interact with the outer surface [25]. Assuming the same mechanism in Be co-deposits, we can explain the lack of the influence of He on D retention at higher deposition temperatures. Since D atoms themselves create the interconnected structures, the inclusion of He does not play an important role. Therefore, we see no difference in D retention when using pure D or $D - 0.1He$ plasma at higher deposition temperatures.

Even though we measured no He desorption in the case of deposition at room temperature, we observed a measurable effect of He on D retention. Therefore, we can assume that the maximal temperature of 1273 K was simply too low for any He desorption from the created co-deposited layer. In the case of higher deposition temperatures at least two desorption peaks are clearly visible in our temperature range. The low temperature peak decreases with deposition temperature, which is an expected behavior since the trap is less populated at higher temperature. On the contrary, the high

temperature peak initially increases with deposition temperature and then decreases for the deposition temperature of 475 K, when also another lower temperature peak appears. The high temperature peak coincides with the desorption around 900 K observed by Eleveld et al. [26], where TDS was performed after He ions were implanted into the Be samples. At 900 K the He-vacancy complex dissociates in Be and leads to an extensive He bubble growth [24]. He is not released until the bubbles are extended to the surface [26], which can occur already around 900 K for our thin layers. The absence of He desorption for the deposition at room temperature is not clear and additional experiments are needed to investigate this desorption behavior.

5. Conclusion

The PISCES-B linear plasma device was used to simulate the creation of Be-D-He co-deposited layers similar to those which are expected to form in the ITER divertor area. The influence of He on D retention in these layers was studied for different deposition temperatures and He concentrations in $D-\alpha He$ plasma, which was used to create the co-deposits. A noticeable effect of He on D retention was observed at lower deposition temperatures when 10% of He was included in the plasma, namely the reduction of D retention is 21% and 36% for deposition at 295 K and 375 K, respectively. For higher deposition temperatures the effect of He is diminished. This behavior is in agreement with the prior data on bulk Be found in the literature, however the effect of He on D retention in Be co-deposits is smaller compared to bulk Be. For lower He concentrations an increase in D retention was observed for the deposition at room temperature, however the difference between pure D and $D - 0.05He$ plasma is less than the uncertainties of the measured data. If we assume that the main net Be deposition zone in ITER will be on inner and outer divertor baffles with the surface temperature of about 388 K, we can predict that He co-deposition can have a favorable influence on hydrogen isotope retention, if He concentration in the plasma is 10% and PISCES-B conditions successfully mimic those of the real ITER divertor. However, He concentration in ITER is expected to be below 6%. Our results show that hydrogen isotope retention could be enhanced for low He concentrations (around 1%) or may not be strongly affected if He concentration reaches the values around 5%, however these results apply only to deposition at room temperature and not at ITER relevant temperature ($\approx$ 400 K).

ACKNOWLEDGMENT

This work has been carried out within the framework of the EUROfusion Consortium and has received funding from the Euratom research and training programme 2014-2018 under grant agreement No 633053. This work was done within the EUROfusion work package PFC. The views and opinions expressed herein do not necessarily reflect those of the European Commission. This work was also supported by the U.S. Department of Energy grant #DE-FG02-07ER54912.

References

[1] S. Brezinsek, A. Widdowson, M. Mayer, V. Philipps, P. Baron-Wiechec, J. W. Coenen, K. Heinola, A. Huber, J. Likonen, P. Petersson, M. Rubel, M. F. Stamp, D. Borodin, J. P. Coad, A. G. Carrasco, A. Kirschner, S. Krat, K. Krieger, B. Lipschultz, Ch. Linsmeier, G. F. Matthews, K. Schmid, JET contributors, Beryllium migration in JET ITER-like wall plasmas, Nucl. Fusion 55 (2015) 063021.

[2] K. Schmid, M. Reinelt, K. Krieger, An integrated model of impurity migration and wall composition dynamics for tokamaks, J. Nucl. Mater. 415 (2011) S284.

[3] K. Schmid, K. Krieger, S. W. Lisgo, G. Meisl, S. Brezinsek, JET Contributors, WALLDYN simulations of global impurity migration in JET and extrapolations to ITER, Nucl. Fusion 55 (2015) 053015.

[4] M.-H. Aumeunier, M. Kočan, R. Reichle, E. Gauthier, Impact of reflections on the divertor and first wall temperature measurements from the ITER infrared imaging system, Nucl. Mater. Energy 12 (2017) 1265.

[5] A. S. Kukushkin, H. D. Pacher, V. Kotov, G. W. Pacher, D. Reiter, Finalizing the ITER divertor design: The key role of SOLPS modeling, Fusion Eng. Des. 86 (2011) 2865.

[6] S. Brezinsek, T. Loarer, V. Philipps, H. G. Esser, S. Grünhagen, R. Smith, R. Felton, J. Banks, P. Belo, A. Boboc, J. Bucalossi, M. Clever, J. W. Coenen, I. Coffey, S. Devaux, D. Douai, M. Freisinger, D. Frigione, M. Groth, A. Huber, J. Hobirk, S. Jachmich, S. Knipe, K. Krieger, U. Kruezi, S. Marsen, G. F. Matthews, A. G. Meigs, F. Nave,

I. Nunes, R. Neu, J. Roth, M. F. Stamp, S. Vartanian, U. Samm, JET EFDA contributors, Fuel retention studies with the ITER-Like Wall in JET, Nucl. Fusion 53 (2013) 083023.

[7] J. Roth, E. Tsitrone, A. Loarte, Th. Loarer, G. Counsell, R. Neu, V. Philipps, S. Brezinsek, M. Lehnen, P. Coad, Ch. Grisolia, K. Schmid, K. Krieger, A. Kallenbach, B. Lipschultz, R. Doerner, R. Causey, V. Alimov, W. Shu, O. Ogorodnikova, A. Kirschner, G. Federici, A. Kukushkin, EFDA PWI Task Force, ITER PWI Team, Fusion for Energy, ITPA SOL/DIV, Recent analysis of key plasma wall interactions issues for ITER, J. Nucl. Mater. 390-391 (2009) 1.

[8] R. A. Causey, D. S. Walsh, Codeposition of deuterium with beryllium, J. Nucl. Mater. 254 (1998) 84.

[9] G. De Temmerman, M. J. Baldwin, R. P. Doerner, D. Nishijima, K. Schmid, An empirical scaling for deuterium retention in co-deposited beryllium layers, Nucl. Fusion 48 (2008) 075008.

[10] G. De Temmerman, R. P. Doerner, Revised scaling equation for the prediction of tritium retention in beryllium co-deposited layers, Nucl. Fusion 49 (2009) 042002.

[11] M. J. Baldwin, T. Schwarz-Selinger, R. P. Doerner, Experimental study and modelling of deuterium thermal release from Be-D co-deposited layers, Nucl. Fusion 54 (2014) 073005.

[12] M. Miyamoto, D. Nishijima, M. J. Baldwin, R. P. Doerner, A. Sagara, Microstructure and deuterium retention of beryllium co-deposition layer formed under high density plasma exposure, Nucl. Mater. Energy 12 (2017) 633.

[13] A. S. Kukushkin, H. D. Pacher, G. Janeschitz, A. Loarte, D. P. Coster, G. Matthews, D. Reiter, R. Schneider, V. Zhogolev, Basic divertor operation in ITER-FEAT, Nucl. Fusion 42 (2002) 187.

[14] S. H. Kim, F. M. Poli, F. Koechl, E. Militello-Asp, A. R. Polevoi, R. Budny, T. A. Casper, A. Loarte, T. C. Luce, Y.-S. Na, M. Romanelli, M. Schneider, J. A. Snipes, P. C. de Vries, The ITPA Topical Group on Integrated Operation Scenarios, Development of ITER non-activation phase operation scenarios, Nucl. Fusion 57 (2017) 086021.

[15] M. J. Baldwin, T. Schwarz-Selinger, R. P. Doerner, D retention in Be exposed to fusion relevant mixed species D_2-He plasma, Nucl. Mater. Energy 12 (2017) 678.

[16] D. Alegre, M. J. Baldwin, M. Simmonds, D. Nishijima, E. M. Hollmann, S. Brezinsek, R. P. Doerner, A parametric study of helium retention in beryllium and its effect on deuterium retention, Phys. Scr. T170 (2017) 014028.

[17] R. P. Doerner, M. J. Baldwin, K. Schmid, The Influence of a Beryllium Containing Plasma on the Evolution of a Mixed-Material Surface, Phys. Scr. T111 (2004) 75.

[18] D. Nishijima, R. P. Doerner, M. J. Baldwin, E. M. Hollmann, R. P. Seraydarian, Spectroscopic determination of the singly ionized helium density in low electron temperature plasmas mixed with helium in a linear divertor plasma simulator, Phys. Plasmas 14 (2007) 103509.

[19] R. P. Doerner, S. I. Krasheninnikov, K. Schmid, Particle-induced erosion of materials at elevated temperature, J. Appl. Phys. 95 (2004) 4471.

[20] M. J. Baldwin, K. Schmid, R. P. Doerner, A. Wiltner, R. Seraydarian, Ch. Linsmeier, Composition and hydrogen isotope retention analysis of co-deposited C/Be layers, J. Nucl. Mater. 337-339 (2005) 590.

[21] G. De Temmerman, M. J. Baldwin, R. P. Doerner, D. Nishijima, R. Seraydarian, K. Schmid, Insight into the co-deposition of deuterium with beryllium: Influence of the deposition conditions on the deuterium retention and release, J. Nucl. Mater. 390-391 (2009) 564.

[22] W. Eckstein, Calculated Sputtering, Reflection and Range Values, IPP-Report 9/132, Max-Planck-Institut für Plasmaphysik, Garching, Germany (June 2002).

[23] M. Tokitani, M. Miyamoto, S. Masuzaki, Y. Fujii, R. Sakamoto, Y. Oya, Y. Hatano, T. Otsuka, M. Oyaidzu, H. Kurotaki, T. Suzuki, D. Hamaguchi, K. Isobe, N. Asakura, A. Widdowson, M. Rubel, JET Contributors, Micro-/nano-characterization of the surface structures on the divertortiles from JET ITER-like wall, Fusion Eng. Des. 116 (2017) 1.

[24] V. N. Chernikov, H. Ullmaier, A. P. Zakharov, Gas bubbles in beryllium implanted with He ions at temperatures $\leq$ 700 K and after post-implantation annealing, J. Nucl. Mater. 258-263 (1998) 694.

[25] V. Kh. Alimov, V. N. Chernikov, A. P. Zakharov, Depth distribution of deuterium atoms and molecules in beryllium implanted with D ions, J. Nucl. Mater. 241-243 (1997) 1047.

[26] H. Eleveld, A. van Veen, F. Labohm, M. W. de Moor, Thermal desorption of helium irradiated beryllium studied by THDS, NDP, PA and SEM, J. Nucl. Mater. 212-215 (1994) 971.